

Quantification of Posterior Capsular Opacification in Digital Images after Cataract Surgery

Sarah A. Barman,¹ Emma J. Hollick,² James F. Boyce,² David J. Spalton,² Bunyarit Uyyanonvara,¹ Giorgia Sanguinetti,¹ and William Meacock²

PURPOSE. To describe a software program developed to provide an objective assessment of the amount of posterior capsular opacification (PCO) in high-resolution digital images of the posterior capsule after cataract surgery.

METHODS. Images are analyzed by a set protocol of defining the area of the posterior capsule, removing the Purkinje light reflexes by intensity segmentation, contrast enhancement, filtering to enhance low-density PCO, and variance analysis using a co-occurrence matrix to assess texture. The accuracy of the system was tested for validity and repeatability.

RESULTS. The software developed has been demonstrated to be an objective method of quantifying PCO. In validation tests, the image analysis-derived measure of PCO showed good agreement with clinically derived measures of PCO. Clinicians assessed PCO on a computer screen image and also under slit lamp examination (Pearson correlation coefficient for both methods >0.92). The entire acquisition and analysis system was demonstrated to have a confidence limit for 2 SDs of 9.8% for group data.

CONCLUSIONS. This system is capable of producing an accurate and reproducible measure of PCO that is relevant to assessing techniques of PCO prevention. (*Invest Ophthalmol Vis Sci.* 2000;41:3882-3892)

Posterior capsular opacification (PCO) is the most common complication of modern cataract surgery, with an incidence of 20%-50%.¹ It is caused by residual lens epithelial cells that remain in the capsular bag after surgery and undergo proliferation, migration, and fibrous metaplasia. This leads to progressive loss of transparency of the posterior capsule and causes visual morbidity when the visual axis is affected. Although it is easy to clear the visual axis by Nd:YAG laser capsulotomy, this is not without complications, which include damage to the intraocular lens (IOL), intraocular pressure elevation, cystoid macular edema, retinal detachment, IOL subluxation, and exacerbation of localized endophthalmitis.²⁻⁴ Laser capsulotomy is expensive, and in the United States it is the second most common surgical procedure reimbursed by Medicare.⁵ Ensuring that elderly patients receive treatment can be difficult, and PCO is a major bar to IOL implantation in developing countries. Consequently, there is considerable interest in techniques to limit PCO. To assess these techniques, a system for its accurate and objective evaluation is required.

Nd:YAG capsulotomy rates have commonly been used as a measure of PCO, but these are a poor method of assessment, because they are subjective and dependent on when the patient asks for treatment and the surgeon offers it, as well as

equipment availability and financial factors. Clinical scoring systems depend on the experience of the examiner and are subjective and qualitative.^{6,7} Retroillumination images can provide an objective way of examining the posterior capsule to give a measurement of PCO. Previous systems had the drawback of being film based, which requires even illumination, consistent processing, and a panel of experienced assessors to grade the image.^{8,9} This type of system has recently been refined by scanning color photographs into a computer and using a mouse and a graphics software package to manually outline and grade the area of opacity.¹⁰

The theoretical advantage of using computer software to analyze images is that observer bias can be reduced and accuracy increased. PCO can take 1 to 3 years before vision is affected. Image analysis offers the potential to shorten the follow-up time for studies of PCO prevention strategies. Retroillumination imaging systems have been used for the assessment of cataract by intensity thresholding, in which the gray scale value of each pixel under scrutiny is used to determine whether it is clear or opaque.^{11,12} This method requires the change from clear to opaque to be defined individually for each pixel relative to background illumination. It creates problems, in that retroillumination images have inherently uneven backgrounds within and between individuals caused by different degrees of pupil dilation, fundus pigmentation, and uneven reflectance from the retina and optic disc, which have to be compensated for by image manipulation. Intensity thresholding is accurate only when the transition from clear to opaque changes the image from light to dark. Intensity thresholding fails in areas of early lens epithelial proliferation where the image is of intensity similar to that of the clear areas, or in more advanced cases in which the thickness of the opacification causes internal reflection and highlights (Fig. 1). This, combined with the necessity for correction of the variation in

From the ¹Medical Imaging Unit, Department of Physics, Kings College; and the ²Department of Ophthalmology, St. Thomas' Hospital, London, United Kingdom.

Supported by a grant from the Iris Fund for Prevention of Blindness and an unrestricted research grant from Alcon Laboratories, Fort Worth, Texas.

Submitted for publication November 15, 1999; revised March 15 and June 6, 2000; accepted June 9, 2000.

Commercial relationships policy: C (DJS, JFB); N (all others).

Corresponding author: David J. Spalton, St. Thomas' Hospital, Lambeth Palace Road, London SE1 7EH, UK.

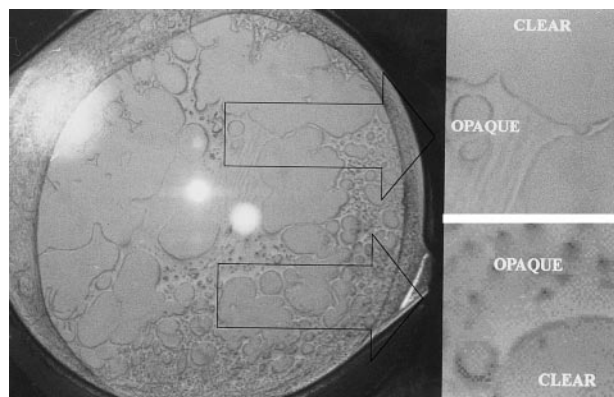


FIGURE 1. Raw image with expanded views of clear and opaque areas showing that areas of opacity can have either higher or similar background intensity to clear areas.

background illumination and the low resolution of some imaging systems, leads to difficulty in accurate assessment of PCO.

We have recently developed a retroillumination camera that produces high-resolution digital images of the posterior capsule. The images have a shallow depth of focus with even and consistent background illumination that can demonstrate the proliferation of lens epithelial cells in the pseudophakic eye.¹³⁻¹⁵ We have developed software based on texture (i.e., the local variance of pixel intensity) to analyze these images to provide an objective measure of PCO.^{14,16,17} In this article we describe the software (the posterior capsule opacity [POCO] software system) and report the validity and reproducibility of the system.

METHODS

The study was approved by the Hospital Ethics Committee, and all patients gave informed consent in accordance with the Declaration of Helsinki.

Image Acquisition

The St. Thomas' Hospital digital retroillumination camera system obtains evenly illuminated images of the posterior capsule through a dilated pupil and stores the images on computer.¹³ The settings in the camera system of flash intensity, beam width, camera aperture, and shutter speed are fixed and ensure that the exposure is standardized between patients. A digital camera (model DCS 420; Eastman Kodak, Rochester, NY) with a chip size of 1024×1536 pixels captures the image. Each pixel contains 8 bits of useful information with a resolution of 25,000 pixels/mm². The image is checked on the monitor to ensure adequate centration and focusing and is then archived as tagged image files (.tif). Images are transferred from the clinic for analysis using a file-transfer protocol (FTP) site on the Internet.

Image Analysis Overview

The software program is based on TRACEE, a dedicated image analysis program (available at no cost at www.ph.kcl.ac.uk) enhanced with dedicated modules written for specific procedures.

We define the area of interest as that part of the posterior capsule that is behind the optic of the IOL and is not obscured by the anterior capsule. If the capsule lies off the anterior

surface of the implant, then the outer edge of the IOL defines the area. This area is called the mask. All images then undergo a protocol of processing steps with identical parameters for each image, consisting of removal of the Purkinje light reflexes, contrast enhancement, filtering, and texture segmentation. Finally, the co-occurrence matrix is matched to the raw image and the area of opacification converted to binary to provide the percentage of PCO.

Defining the Mask

The mask is defined on a 21-in. monitor using a mouse and a graphic icon to draw around the area of interest. The mask is then saved as a general image file (.gif). Figure 2A shows the raw image of Figure 1 with a mask applied. The area peripheral to this is eliminated from subsequent calculations. The mask area is a useful tool that can be used to assess capsular movement relative to the optic over time or to capsular phimosis or retraction.

Removal of the Purkinje Light Reflexes

The Purkinje light reflexes originate from the cornea and the anterior and posterior IOL surfaces and must be excluded from further analysis. This is performed using segmentation based on intensity values of the image, rather than the texture values required to identify PCO. A full description of the segmentation technique is given later. After the identification of the Purkinje light reflexes, a second mask is generated that blanks off the areas where the image is saturated, and that is combined with the existing mask (Fig. 2B). It is important to use intensity segmentation to identify the Purkinje reflexes rather than simple intensity technique, because, although the central bright reflex could be found easily in this manner, the more diffuse reflexes cannot be adequately identified.

Contrast Enhancement

After the area of interest is defined, the image is contrast enhanced. Instead of applying one particular contrast enhancement function across the entire image, our technique uses a local calculation of the mean \pm SD over a defined area surrounding each pixel.¹⁸

The function applied to the image is given in equation 1, in which w is a square patch area with dimensions of 99×99 pixels. The patch surrounds the pixel under operation. The average intensity within area w is $\langle f \rangle_w$, where f is the value of the pixel intensity that is currently in operation, σ_w is the SD over area w , f_{\min} is the minimum intensity value of the whole image, and f_{\max} is the maximum intensity value of the whole image.

$$f \rightarrow 255[g(f) - g(f_{\min})][g(f_{\max}) - g(f_{\min})]^{-1}$$

where

$$g(f) = [1 + \exp[(\langle f \rangle_w - f)/\sigma_w]]^{-1} \quad (1)$$

Figure 2C shows the contrast-enhanced image of Figure 2B. It is important to mask the Purkinje reflexes before contrast enhancement to avoid shadowing effects surrounding the bright reflections.

Mean Filtering

Some images contain areas of opacification that have texture similar to that of the transparent areas. An example of this type of opacification is shown in the top expanded area of Figure 1.

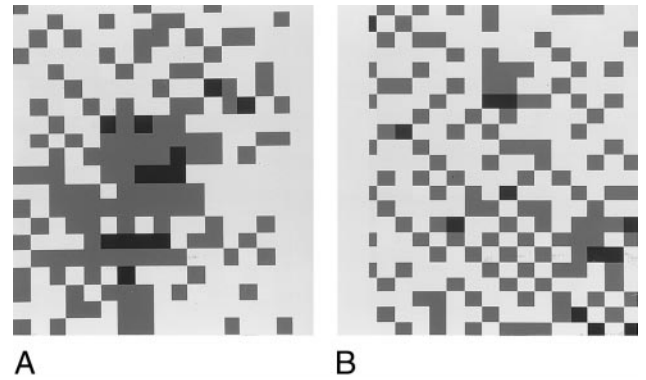
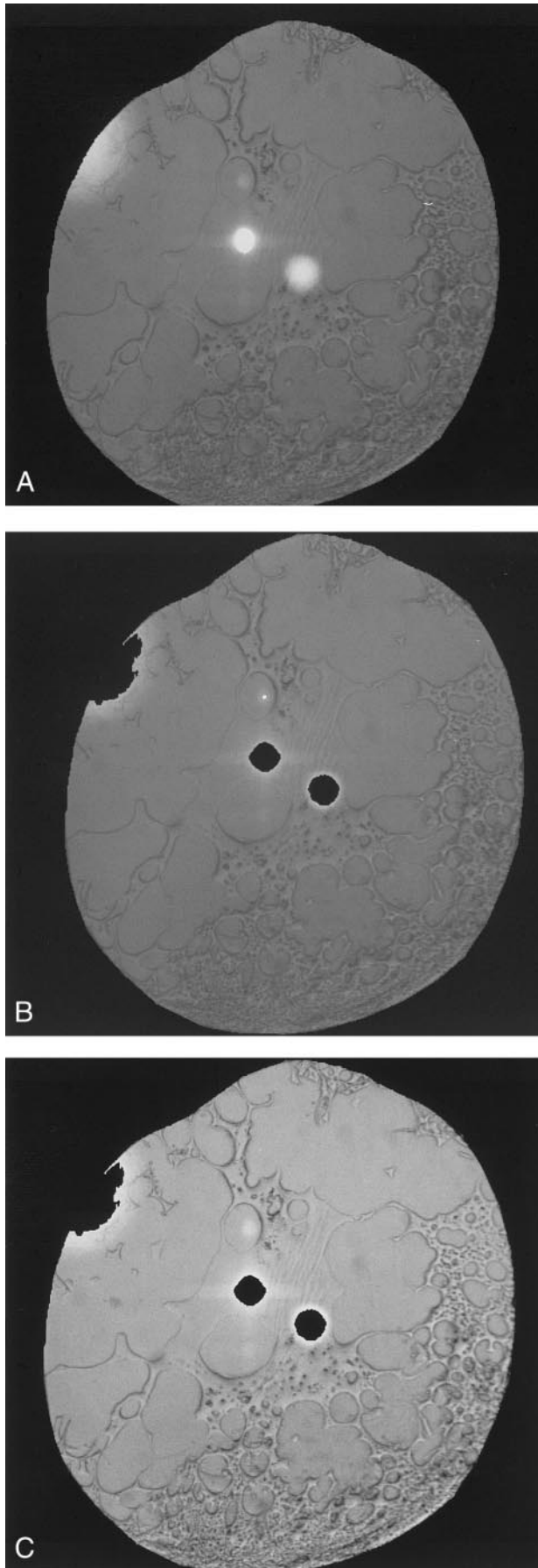


FIGURE 3. (A) Expanded view of opaque area showing that pixel intensity tends to be clumped. (B) Expanded view of transparent area showing individual pixel intensity is more randomly distributed.

It is difficult to identify these areas correctly as transparent or opaque using co-occurrence segmentation. Filtering was developed to enhance the texture of these areas of opacity. Figures 3A and 3B show an example of a faint opaque and a transparent region from Figure 1. The images are shown expanded so that the intensity of the gray levels and their structure are clearly visible. These show that although the overall intensity levels of the opaque and transparent areas are the same, the difference between them is that they are arranged differently. Pixels in the opaque region with similar gray levels are more likely to clump into 10 or more in comparison with those in the transparent region that tend to be more evenly scattered.

This type of texture can be enhanced by the application of a mean filter applied over the entire image. When the individual intensity of a group of pixels is summed, the texture of the gray levels that are present in clumps is enhanced, and the randomly scattered gray levels are reduced to a single average intensity value.

Quantitative experiments were performed to determine the optimal size and type of the filter. Images were selected with substantial areas of early lens epithelial cell proliferation that produced very thin layers of opacification that the texture segmentation found difficult to classify correctly as opaque. Mean and median filters of various sizes were applied to the contrast-enhanced images before the texture segmentation analysis was performed to identify PCO. The percentage area correctly recognized as opaque in the opaque areas was recorded, and in the transparent areas the percentage area correctly recognized as transparent was recorded similarly. The performance of the system as a whole was summarized as a verdict value, defined as a multiplication of the opaque and transparent percentages, scaled to a maximum performance target of 1.

Consideration of the verdict values showed that a mean filter is optimal in comparison with a median filter, and the optimal filter size of filter was shown to be 3×1 pixels. However, this type of filter is asymmetric and may not be appropriate for detecting PCO where there is a strong direc-



FIGURE 2. (A) Raw image with capsule mask applied defining the area of the posterior capsule within the rhexis for further image analysis. (B) Raw image with capsule mask and light reflex mask applied to remove Purkinje light reflexes. (C) Contrast enhancement of the image within the rhexis.

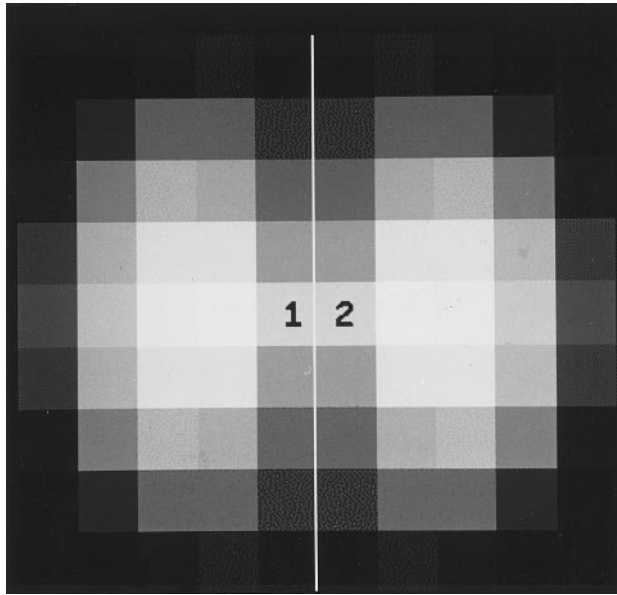


FIGURE 4. Edge filter. This is applied to each pixel in the image, providing a measurement of variance on either side of the pixel.

tional bias (as is the case when there are folds within the capsule). A 4×4 -pixel filter was consistently close in performance to the 3×1 -pixel filter and has the advantage of being less directional. It was therefore judged to be the most appropriate. This result was verified by running the filter on a library of images so that a qualitative judgment could be made on whether the filter improved performance of opacification recognition. Compared with the situation in which the image was left unfiltered, the use of a 4×4 mean filter greatly improved recognition of opaque and transparent regions.

Texture Segmentation

After these preprocessing steps, the image is classified into areas of opacity and transparency using a technique known as image segmentation. An increase in opacification of the posterior capsule is characterized by an increase in the texture (i.e., structural detail) of the image. Paplinski and Boyce¹⁹ have shown that texture performs well as a method of detecting opacification.

If the intensity values vary substantially over an area, that area must be textured. A directional variance filter is applied to the image to extract information on its texture. The region from which the local variance is calculated is asymmetric with a defined directionality, and the values within the region are weighted, resulting in a variance filter.

The structure of the filter is derived from the work of Canny²⁰ on optimized edge operators. To create the two-dimensional filter shown in Figure 4, we initially used a one-dimensional Petrou-Kittler edge filter. This filter is optimized for the ramp edges that are prevalent in our images. To expand this edge filter to two dimensions, a further gaussian filter is applied in the direction orthogonal to the edges to be detected.

Using a complex number notation, the resultant two-dimensional filtering component $b(u)$ used to perform segmentation of the images is of the following form

$$b(u) = \eta \cdot s(r) \cdot p(\vartheta), \quad u = re^{j\vartheta}, \quad p = \exp(c_\vartheta \vartheta^2) \quad (2)$$

where η is the normalization constant, and the pixel vector u is specified by its radial and angular components r and ϑ . The

angular spread of the filter is controlled by the variance parameter c_ϑ , and $s(r)$ represents the form of the Petrou-Kittler one-dimensional edge filter.

This combination of filters produces the bow-tie-shaped filter shown in Figure 4. The long axis of the bow tie is horizontal, and the values recorded for each pixel in the bow tie are weighted relative to its position. The representation of the filter in Figure 4 shows varying gray scales assigned to the surrounding pixels, which represent the weight of the filter given to each of these pixels. Those pixels marked white have the highest weighting.

Each pair of pixels in the image (marked as pixels 1 and 2 in Fig. 4) are assigned two variance values, that of right variance, where the bow-tie-shaped filter extends to the right, and that of left variance, where it extends to the left. The two values of variance give information, not only on the texture values surrounding each pixel, but also on the edge values. Values of the variance calculated by applying the filter to the image are represented as a co-occurrence matrix²¹ that displays the values of variance obtained from the image. Figure 5 shows a typical co-occurrence matrix with a horizontal scale of right variance and a vertical scale for left variance. The largest peak of the co-occurrence matrix (the black region) represents the transparent, low-textured region, whereas the dark gray area represents the wide range of textured regions associated with opaque areas of the posterior capsule. The square root of the matrix shown in Figure 5 has been calculated three times so that the detail of the matrix may be viewed more clearly.

Analysis of the Co-occurrence Matrix

To separate the image into two classes (opaque and clear) the surface of the co-occurrence matrix (which may be thought of as a contour map) is examined, and a series of gaussian distributions are fitted to the surface of the matrix using the expectation maximization algorithm.²² This algorithm iteratively maximizes the log likelihood of the allocation of the data (within the co-occurrence matrix) to the gaussian distributions. The method alternates the most likely allocation of the

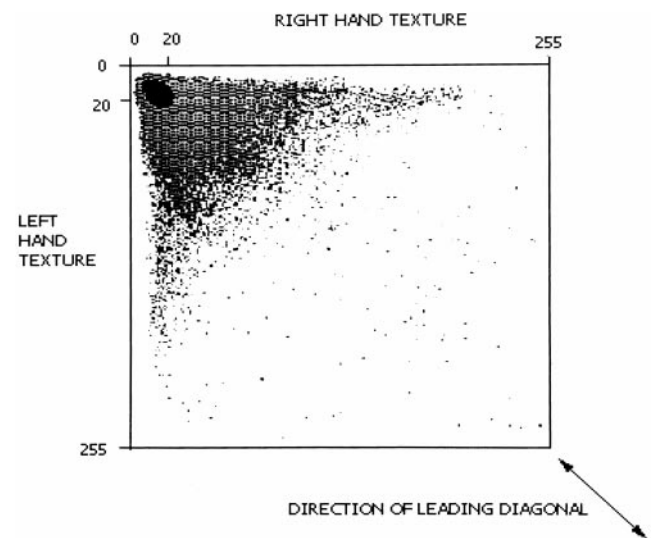


FIGURE 5. Co-occurrence matrix plotting the righthand versus left-hand variance of each pixel in the image. The black area in the top left corner represents transparent pixels.

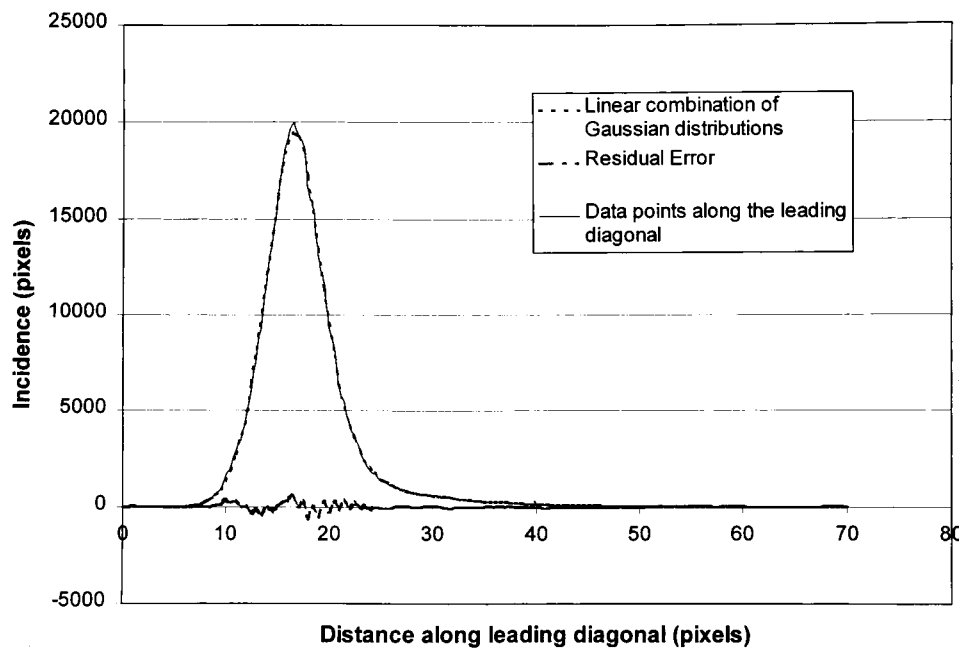


FIGURE 6. Leading diagonal of co-occurrence matrix. The *horizontal axis* represents the distance along the leading diagonal of the co-occurrence matrix (a limited range of the full 256 elements is shown). The *vertical axis* represents the incidence of pixels within the co-occurrence matrix. The *solid line* shows the original representation of the leading diagonal of the co-occurrence matrix. The *dashed peak* shows a linear combination of distributions fitted to the original peak. The *dotted line* running along the bottom of the graph represents the small error between the original and gaussian fit.

data with the determination of the most likely values of the parameters of the distributions.

Although the gaussian distributions are fitted over the entire surface of the matrix, the leading diagonal is a useful area to analyze to assess the accuracy to which the gaussian distributions have been fitted. Figure 6 shows a graph representing the leading diagonal of the co-occurrence matrix of Figure 5. The solid line represents the peak within the co-occurrence matrix (shown in black on Fig. 5). The dashed peak shows a linear combination of distributions fitted to the original peak. The dotted line running along the bottom of the graph represents the error between the original and gaussian fit and shows a low residual error due to noise and the peak of the co-occurrence matrix not being exactly gaussian in shape.

The expectation maximization algorithm fits a number of different gaussian distributions to the surface of the co-occurrence matrix. The number of distributions depends on the complexity of the shape of the surface of the co-occurrence matrix. Typically, the algorithm fits five gaussian distributions, which are used to construct the final segmentation. From the classification of the co-occurrence matrix, each pixel within the image is assigned a class.

The classes that correspond to the opaque areas of the image are grouped together, and those that correspond to transparent areas are grouped to produce a simple black-and-white classification of the image. Figure 7 shows the final segmentation of Figure 2A. The white area shows the transparent regions of the posterior capsule, the black area shows the opaque regions, and the gray area shows the area outside the mask and the Purkinje light reflexes that are excluded from the analysis. A visual inspection indicates that the segmentation matches both the transparent and opaque regions of the raw image to a high degree of accuracy. The final output of this program is a calculation of the percentage area of opacification based on the number of opaque pixels within the mask area compared with the total number of pixels within the mask area, in the case of Figure 7 giving a value of 64% opacification. Figures 8A and 8B and

Figures 9A and 9B demonstrate eyes with less (45%) and more (89%) opacification.

Validity of the System

Two data sets were used to test the validity of the image analysis system. The validity of the system was determined by comparing clinically derived measures of the PCO with an image analysis-derived measure using the POCO software system.

To assess the ability of the computer image analysis system to recognize clinical PCO, two independent experienced and masked clinicians viewed 24 patients on the slit lamp and estimated the percentage PCO on the posterior capsule. The clinical results were compared with the percentage-derived computer segmentation performed later by an independent masked operator.

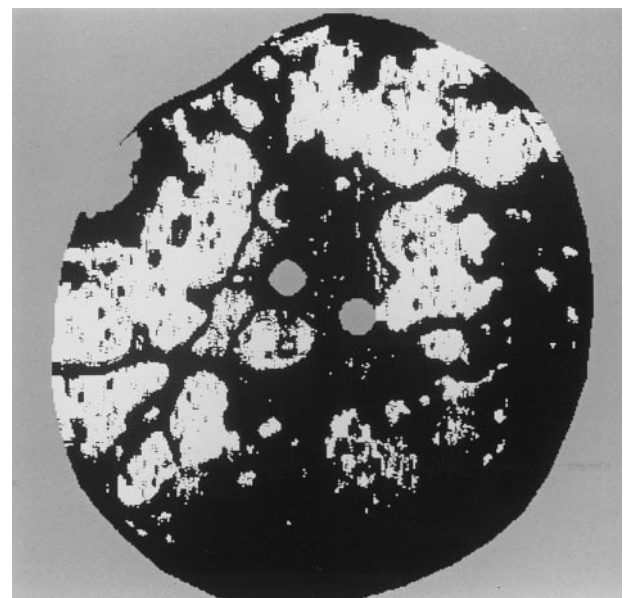


FIGURE 7. Final segmentation showing an area of 64% opacification.

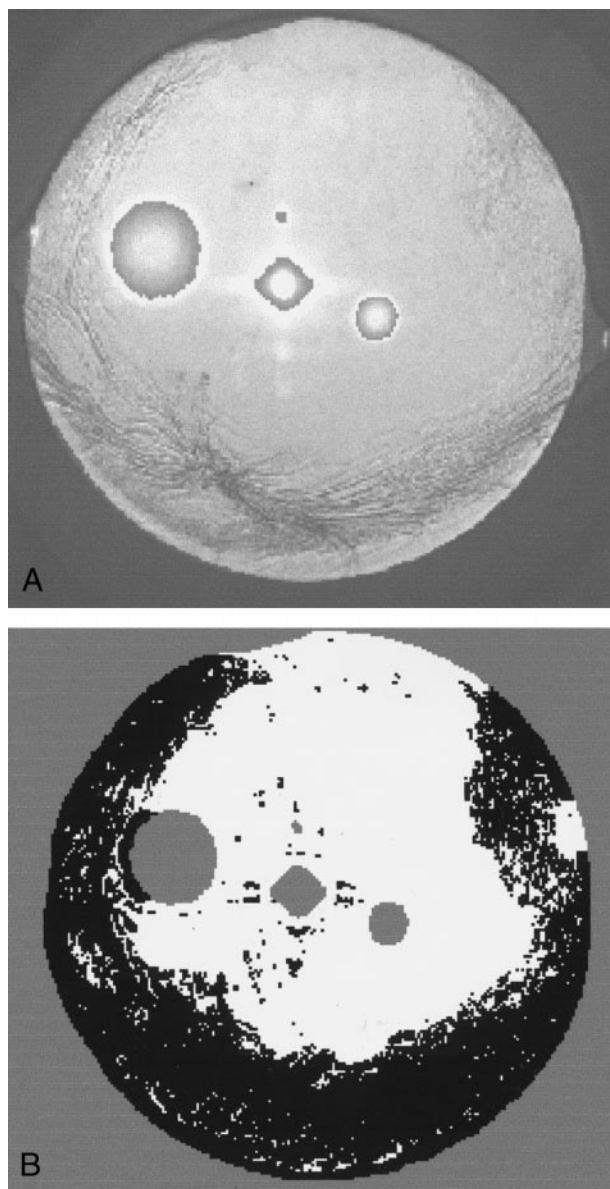


FIGURE 8. (A) Contrast-enhanced image. (B) Segmented image of (A) showing an area of 45% PCO.

The validity of the findings of the computer image analysis system in recognizing PCO in the retroillumination images was assessed by three experienced clinicians who independently viewed 30 retroillumination images chosen to represent the complete spectrum of PCO from zero to complete PCO. The images were viewed by the clinicians on a computer monitor and scored for percentage of PCO coverage. Results were compared with the percentage of PCO derived independently by the masked computer operator.

Repeatability of the System

A third data set was used to assess the repeatability of the entire image acquisition and analysis system, consisting of images of 32 eyes of individual patients taken 1 week apart. The data set included equal numbers of patients exhibiting mild, moderate, and severe opacification. Images were taken 1 week apart, because over a week, the degree of PCO would be

unlikely to change but head position, fixation, pupil dilation, and focus could vary.

Interoperator Reproducibility of the System

A fourth set of 30 images were analyzed by two different operators under double-masked conditions to assess the interoperator reproducibility of the image analysis software. Potential operator-dependent variables are the definition of the mask area and the final segmentation of the image that is partly operator dependent, because one of a given set of presented possibilities must be selected.

All the four data sets used in these tests were from separate groups of patients. Except for the slit lamp validation set, in which two of the patients had both eyes photographed, all other patients in the four data sets had just one eye photographed. The age of the patients in all four data sets ranged from 50 to 80 years.

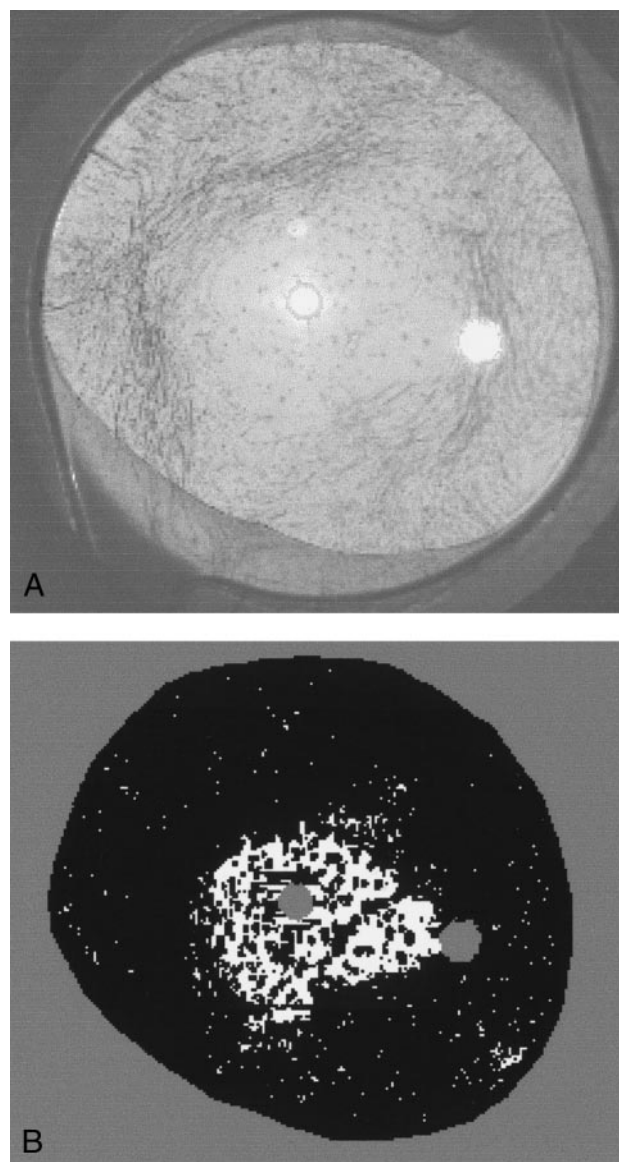


FIGURE 9. (A) Contrast-enhanced image. (B) Segmented image of (A) showing an area of 89% PCO.

Statistics

All the data were analyzed using commercial software (Excel; Microsoft, Redmond, WA). The Pearson correlation coefficient (r) was calculated to test the validation and the repeatability of the system. The Bland-Altman²³ method of assessing agreement between two methods of clinical measurement was used to analyze repeatability.

RESULTS

Validity

The image analysis-derived measure of opacification and the slit lamp-derived estimation of opacification showed

good agreement. The results are shown in Figure 10: $r > 0.96$ when both of the clinical values were correlated with the image analysis POCO software system. When the means of the clinical values were correlated with the values from the software, $r = 0.98$.

Agreement was also good between the estimate of the clinicians of PCO when the retroilluminated images were viewed on the computer monitor in the image analysis software system. The results are shown in Figure 11: $r > 0.92$ for all three clinical values when correlated with the image analysis software system. When the means of the clinical values were correlated with the software values, $r = 0.95$.

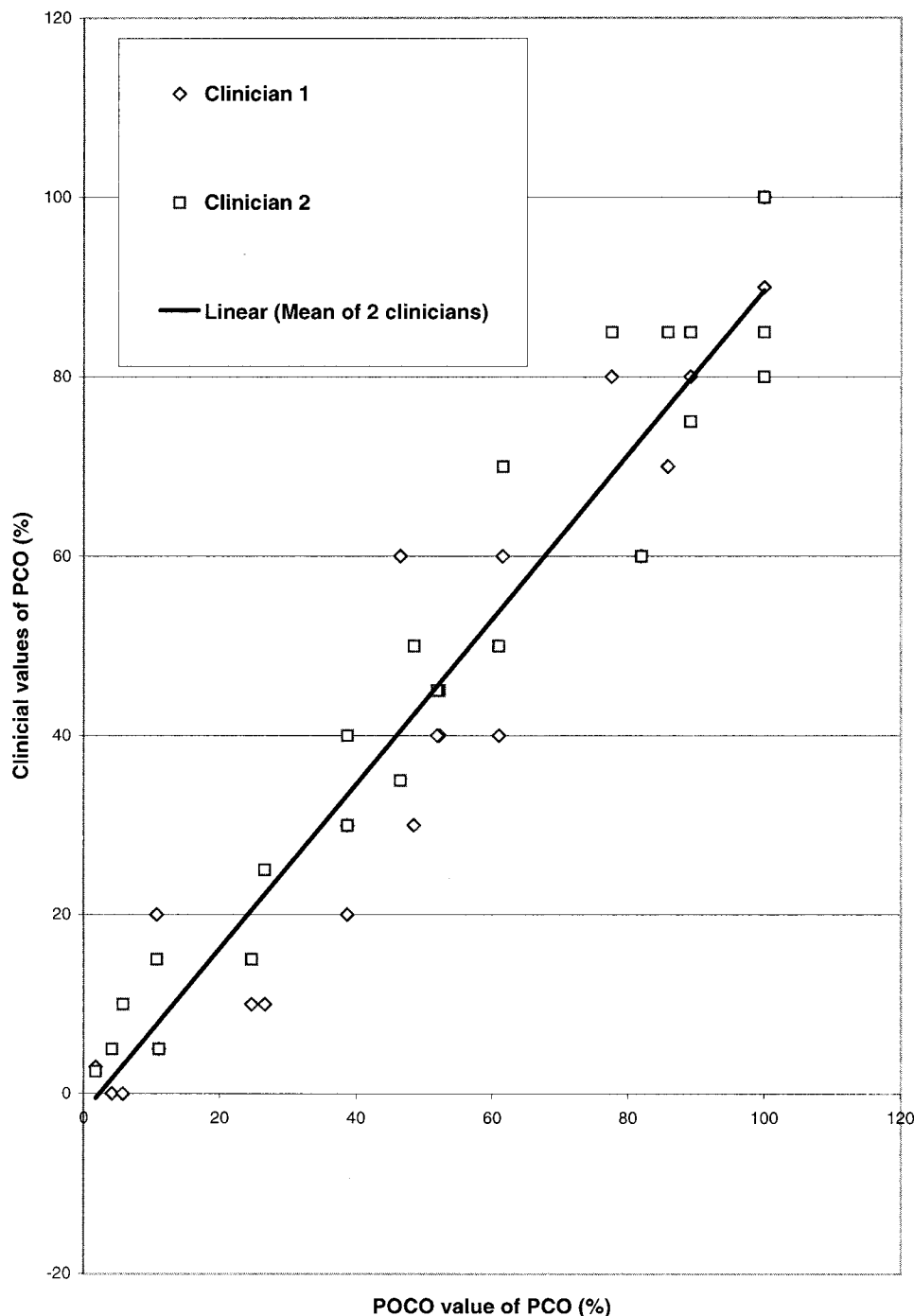


FIGURE 10. Comparison of findings of two clinicians (grading on slit lamp examination) versus those of the POCO image analysis software system. The trendline is a linear least mean squares fit to the mean of the clinicians' values ($r = 0.98$).

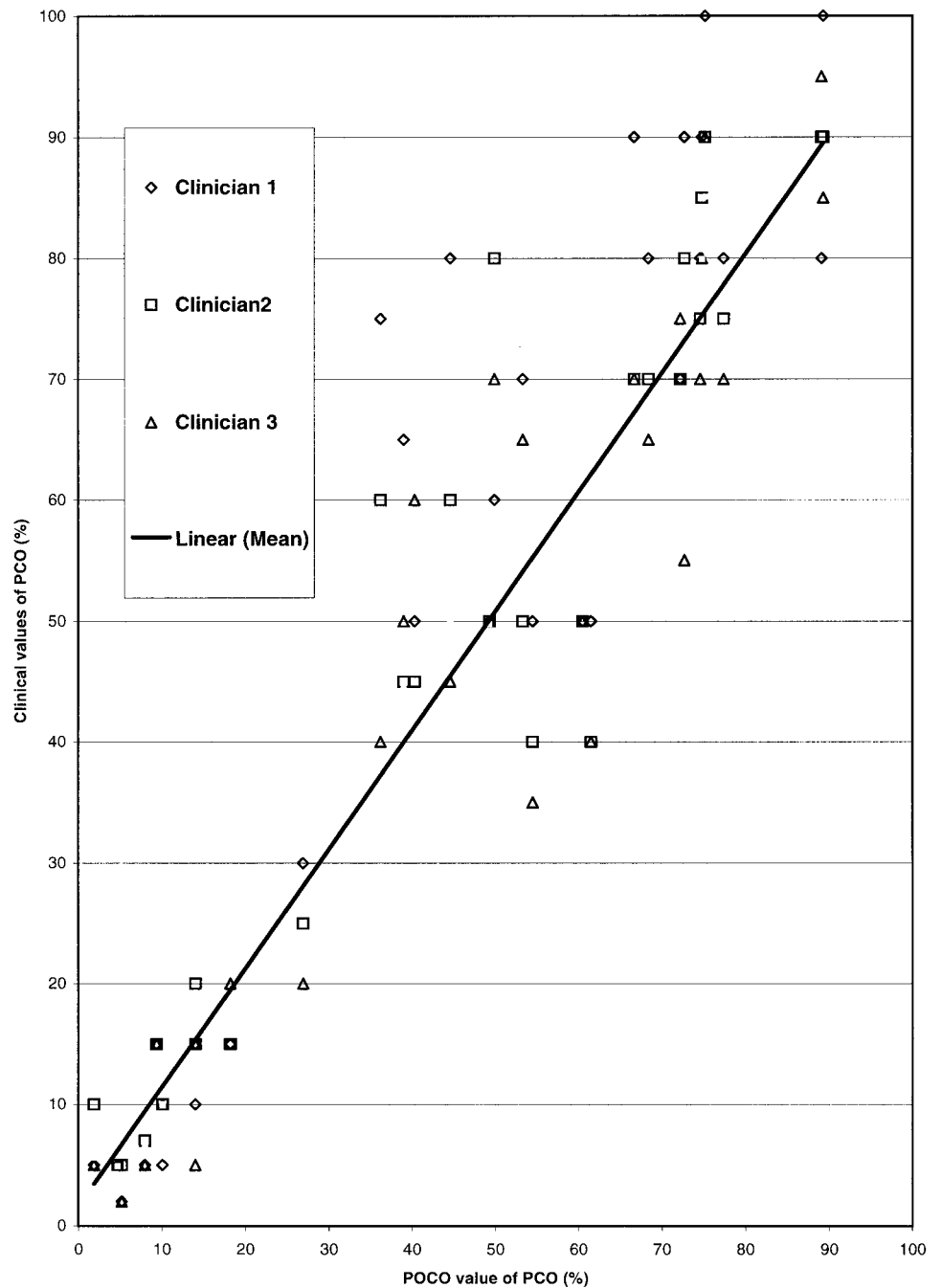


FIGURE 11. Comparison of findings of three clinicians (viewing retroillumination images on computer monitor) versus those of the POCO image analysis software system. The trend-line is a linear least mean squares fit to the mean of the clinicians' values ($r = 0.95$).

Repeatability of the System

Thirty-two patients had two images taken 1 week apart (Fig. 12; $r = 0.99$). The mean difference of the two sets of results was -0.33% . The SD of the differences was 4.70% . From this we derived the 95% limits of agreement, which were $+9.1\%$ and -9.8% . The method is therefore repeatable to within 9.8% for group data of 30 patients.

Interoperator Reproducibility

The interoperator reproducibility test on 30 images between two operators showed good agreement (Fig. 13; $r = 0.99$).

DISCUSSION

We describe a method of objectively measuring PCO in retroillumination images using image analysis based on texture segmentation. The findings correlate well with clinical estimation of PCO and have low operator error and good reproducibility. We have used this technique successfully to quantify PCO with different intraocular lenses and surgical techniques.^{14,16,17}

Nd:YAG laser capsulotomy rates have been used in many studies to compare the influence of various factors on PCO. These are subjective and also only give an indication of opacification that affects vision. It usually takes several years for PCO to develop to such a degree after surgery means that long-term follow-up is required before the influence of factors on PCO is

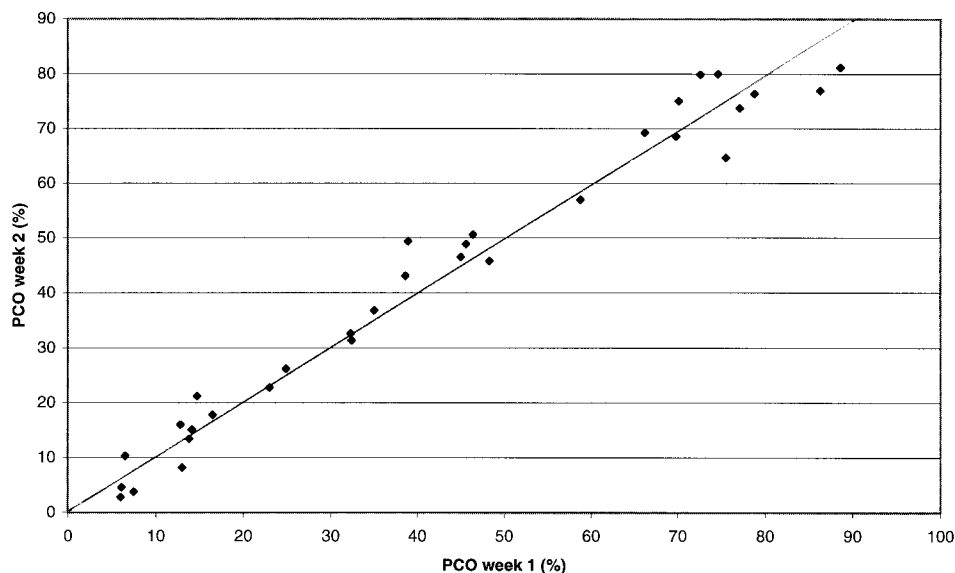


FIGURE 12. Comparison of images taken 1 week apart and analyzed on the POCO software system ($r = 0.99$).

known. Many attempts have therefore been made to provide a more objective method of assessment. Apart from one technique that relies on backscattering of light,²⁴ these have all used retroillumination imaging of the posterior capsule.¹⁰⁻¹² For image analysis the raw image must be of the highest quality possible with high resolution, correct exposure, focus, and even illumination, because the analysis cannot compensate for information that is not present. Our system has been purposely designed to meet these criteria. Direct image acquisition allows image quality to be checked immediately, and the system has a resolution of 25,000 pixels/mm².

The analysis of retroillumination images presents unique problems: They are of low contrast, with complex features and indistinct and incomplete boundaries. A simple overlay grid scoring system²⁵ has been used. A more sophisticated system uses computer graphics to outline areas of opacity on color images.¹⁰ This, however, relies on a skilled operator to outline the areas of opacity that can have complex honeycomb features (Fig. 1). Intensity thresholding is a

simple image analysis technique that requires each pixel in the image to be assigned a gray-scale value. This is compared with a baseline measurement, and pixels darker than this threshold are defined as opaque. This method has been used successfully in the Oxford Cataract Camera (Marcher Enterprises, Hereford, UK) and the Nidek Anterior Segment Analyser (Nidek, Gamagori, Japan) to quantify cataract. We have tried this technique to measure PCO and have found that it has serious inherent problems. Pixel intensity depends on the degree of illumination that itself is dependent on such variables as pupillary dilation, fundus pigmentation, or artifacts from fixation off the visual axis so that substantial variations can occur across an image or between consecutive images. Measurement of opacification requires the definition of the threshold at which the change from clear to opaque occurs, and small changes in this can cause wide variations. A method using software to compensate for changes in illumination has recently been described.¹² However, many images also contain areas of PCO with intensity

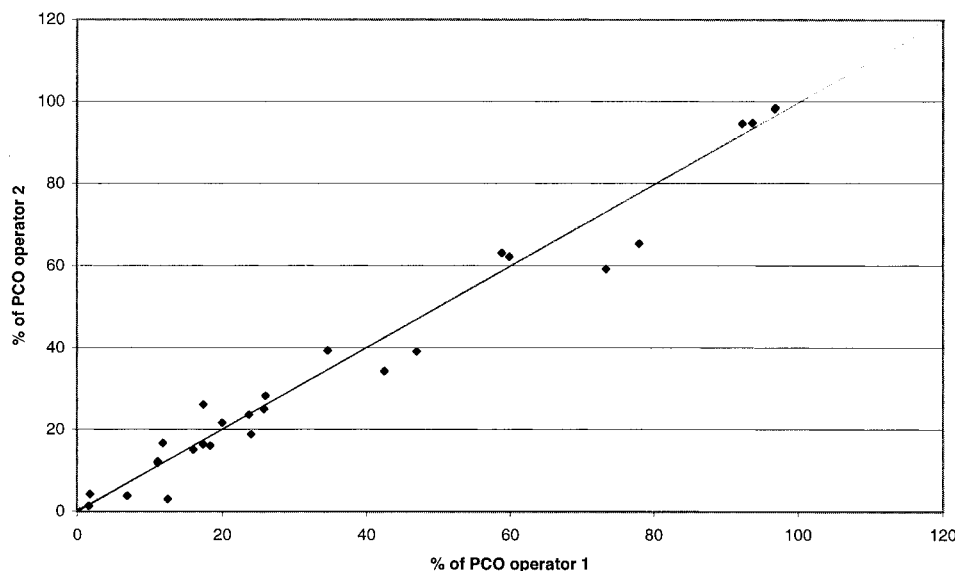


FIGURE 13. Summary of interoperator results. Images were analyzed by two computer operators using the POCO software system ($r = 0.99$).

values of levels similar to that in clear areas, or images may have brighter values than clear areas due to reflection of light within the thickness of the lens epithelial cell membrane (Fig. 1). Intensity thresholding cannot deal, by definition, with these situations.

These problems are resolved by using measures of texture for the analysis that are independent of illumination. Texture is a measure of the variation of intensity between a given pixel and its adjacent files. Opacification is characterized by an increase in texture, whereas clear areas are featureless. This article has shown that this works well in clinical practice. The major disadvantage is that the software programs for this system are sophisticated and require considerable computing capacity. However, despite the computing capacity required, the system is reasonably fast and simple to operate. The image analysis procedure requires operator input for approximately 2 minutes with a processing time of approximately 3 minutes, so that an image can be analyzed in approximately 5 minutes. The program runs on a workstation (02 1200MHz; Silicon Graphics, Mountain View, CA) under a UNIX environment. An operator can be trained to use the system in 2 to 3 weeks. Approximately 2 to 3 weeks' training is also required for training the photographer to obtain high-quality retroillumination images, but once this is accomplished, images are acquired in less than 5 minutes.

We found a high degree of correlation between experienced clinicians viewing PCO on the slit lamp or the contrast-enhanced image and the area of PCO derived by the software program. The human eye is extremely good at detecting PCO, especially when the image can be viewed on a computer monitor at leisure, and the contrast enhancement program makes areas of flat plaquelike PCO more apparent. When the capsule is either totally clear or opaque there is, of course, no difficulty in establishing the percentage opacification clinically, but it becomes more difficult and subjective to do this clinically at intermediate percentages when there are complex patterns of lens epithelial cell growth (Fig. 2C).

A major variability in imaging is pupillary dilation. We therefore tested the reproducibility of our system by imaging of the same eye 1 week later, PCO being unlikely to alter in this time, and found an excellent correlation between the first and second images ($r = 0.99$). In another series of images, inter-operator variability was shown to be low. Using the Bland-Altman²³ method of assessing reproducibility there was a confidence limit for 2 SDs of 9.8% for group data on 32 eyes.

Our system has a shallow depth of focus, but any opacity within the focal range will contribute to the retroillumination image. In practice, anterior vitreous opacity does not appear to cause much artifact, but it is important to exclude any patients with severe vitreous or corneal opacity from PCO studies. A major problem with our system is that the Purkinje reflexes lie centrally in the image. Because we use axial illumination, and they are of high intensity, they cannot be removed by polarized filters. We remove them by image processing, and data are lost in these areas. This is an area that we are currently working to improve. Another problem is the definition of the area of PCO to be studied. In this study we defined the posterior capsule as that area lying inside the rhexis or the edge of the lens optic if the rhexis lay off the implant. This has the advantage that early PCO can be detected because it begins in the peripheral areas. Other investigators have used an area centered on the visual axis defined by using either the intraocular lens edge or pupil margin. All these methods have potential pitfalls as the rhexis

size can increase or decrease after surgery, the lens can tilt or decenter, or the pupil may dilate unevenly. Our software has the potential to define a mask based on any of these parameters, and the most suitable can be chosen for a particular study.

Our current program provides an overall percentage of the area of the posterior capsule that is opaque, and this has been a useful tool in investigating various strategies to limit PCO. Ideally, it would be helpful also to have some measure of the severity of PCO, because it is possible to have a thin lens epithelial membrane that covers most of the surface of the posterior capsule and the visual axis without affecting vision. High-percentage opacification measurements do not necessarily correlate with visual function. Visual degradation of the image is produced by forward light scattering into the eye, and areas of PCO that appear to be severe or dense on clinical examination may in fact be less visually damaging than apparently less dense areas, because they attenuate rather than scatter light. We believe therefore, that measurements of PCO severity are misleading unless they are correlated to changes in visual function.

In conclusion, the software described in this article provides an objective and reproducible method to quantify PCO and should prove useful in the investigation of strategies to limit this important complication of cataract surgery.

Acknowledgments

The authors thank Kate Tilling of the Department of Public Health, United Dental and Medical Schools, London, United Kingdom, for statistical advice, Masaki Komine for statistical input, Andrew Paplinski for technical discussions, and Saab Bhermi for clinical input.

References

- Apple DJ, Solomon KD, Tetz MR, et al. Posterior capsular opacification. *Surv Ophthalmol.* 1992;37:73-115.
- Murrill CA, Stanfield DL, Van Brocklin MD. Capsulotomy. *Optom Clin.* 1995;4:69-83.
- Javitt JC, Tielsch JM, Canner JK. National outcomes of cataract extraction: increased risk of retinal complications associated with Nd:YAG laser capsulotomy. *Ophthalmology.* 1992;99:1487-1497.
- Steinert RF, Puliafito CA, Kumar SR, et al. Cystoid macular edema, retinal detachment, and glaucoma after Nd:YAG laser posterior capsulotomy. *Am J Ophthalmol.* 1991;112:373-380.
- Steinberg EP, Javitt JC, Sharkey PD, et al. The content and cost of cataract surgery. *Arch Ophthalmol.* 1993;111:1041-1049.
- Sellman TR, Lindstroem RL. Effect of a plano-convex posterior chamber lens on capsular opacification from Elschmig pearl formation. *J Cataract Refract Surg.* 1988;14:68-72.
- Legler UFC, Apple DJ, Assia EI, et al. Inhibition of posterior capsule opacification: the effect of colchicine in a sustained drug delivery system. *J Cataract Refract Surg.* 1993;19:462-470.
- Hansen S, Solomon K, McKnight G, et al. Posterior capsular opacification and intraocular lens decentration, Part I: comparison of various posterior chamber lens designs implanted in the rabbit model. *J Cataract Refract Surg.* 1988;14:605-613.
- Tetz M, O'Morchoe D, Gwin T, et al. Posterior capsular opacification and intraocular lens decentration, Part II: experimental findings on a prototype circular intraocular lens design. *J Cataract Refract Surg.* 1988;14:614-623.
- Tetz MR, Auffarth GU, Sperker M, et al. Photographic image analysis of posterior capsule opacification. *J Cataract Refract Surg.* 1997;23:1515-1520.
- Vivino MA, Mahurkar, Trus B, et al. Quantitative analysis of retroillumination images. *Eye.* 1995;9:77-84.
- Friedman DS, Duncan DD, Munoz B, et al. Digital image capture and automated analysis of posterior capsular opacification. *Invest Ophthalmol Vis Sci.* 1999;40:8, 1715-1722.

13. Pande MV, Ursell PG, Spalton DJ, et al. High-resolution digital imaging of the posterior lens capsule after cataract surgery. *J Cataract Refract Surg.* 1997;23:1521-1527.
14. Ursell PG, Spalton DJ, Pande MV, et al. Relationship between intraocular lens biomaterial and posterior capsular opacification. *J Cataract Refract Surg.* 1998;24:352-360.
15. Hollick EJ, Ursell PG, Pande M, Spalton DJ. Lens epithelial cell regression on the posterior capsule: a 2 year prospective randomised trial with three different intraocular lens materials. *Br J Ophthalmol.* 1998;82:1182-1188.
16. Hollick EJ, Spalton DJ, Ursell PG, et al. The effect of PMMA, silicone and polyacrylic lenses on posterior capsular opacification three years after cataract surgery. *Ophthalmology.* 1996;106:49-54.
17. Hollick EJ, Spalton DJ, Meacock WR. The effect of capsulorhexis size on posterior capsular opacification: one year results of a randomised prospective trial. *Am J Ophthalmol.* 1998;128:271-279.
18. Sinthanayothin C, Boyce JF, Cook HL, Williamson TH. Automated localisation of the optic disc, fovea and retinal blood vessels from digital fundus images. *Br J Ophthalmol.* 1999;83:8902-8910.
19. Paplinski AP, Boyce JF. Segmentation of a class of ophthalmological images using a directional operator and co-occurrence arrays. *Opt Eng.* 1997;36:3140-3147.
20. Canny J. A computational approach to edge detection. *IEEE Transactions on Pattern Analysis and Machine Intelligence.* 1986;8:679-698.
21. Haralick RM, Shannergarn K, Dinstein I. Textural features for image classification. *IEEE Transactions in Systems, Man and Cybernetics.* 1973:610-621.
22. Titterton AFM, Smith DM, Makov UE. *Statistical Analysis of Finite Mixture Distributions.* London, UK: J. Wiley & Sons 1985.
23. Bland JM, Altman DG. Statistical methods for assessing agreement between 2 methods of clinical measurement. *Lancet.* 1986;1:307-310.
24. Hayashi K, Hayashi H, Nakao F, et al. In vivo quantitative measurement of posterior capsule opacification after extracapsular cataract surgery. *Am J Ophthalmol.* 1998:837-843.
25. Clark DS, Emery JM, Munsell MF. Inhibition of posterior capsule opacification with an immunotoxin specific for lens epithelial cells: 24 months clinical results. *J Cataract Refract Surg.* 1998;24:1614-1620.